Stress Analysis using Diffractive Optic Interferometry

John A. Gilbert
Department of Mechanical and Aerospace Engineering
University of Alabama in Huntsville
Huntsville, Alabama 35899

Robert L. Shepherd
Division of Engineering
Colorado School of Mines
Golden, Colorado 80401

Helen J. Cole
Astrionics Laboratory
NASA Marshall Space Flight Center
MSFC, Alabama 35812

Paul R. Ashley
Weapons Sciences Directorate
U.S. Army Missile Command
Redstone Arsenal, Alabama 35898-5000

David J. Alldredge
Department of Mechanical and Aerospace Engineering
University of Alabama in Huntsville
Huntsville, Alabama 35899

Abstract

Diffractive optic interferometry (DOI) is a technique for measuring both in-plane and out-of-plane displacement with variable sensitivity using the same optical system. Sensitivity is varied by utilizing various combinations of the different wavefronts produced by a conjugate pair of binary optical elements; a transmission grating is used to produce several illumination beams while a reflective grating, replicated on the surface of a specimen, provides the reference for the undeformed state.

Introduction

Many different full-field optical methods have been developed to measure surface displacement, but simultaneous measurement of all three components using the same experimental setup is a rarity. In the few cases where this has been accomplished, there were some disadvantages.

Basehore and Post [1,2], for example, proposed a technique whereby the u and w displacements were recorded together but their approach was complex in that successive optical filtering was required to separate the displacement components. Asundi and Cheung [3,4], and Asundi, Cheung and Lee [5], reported on an approach for simultaneous measurement of u, v, and w; however, the images recorded for in-plane and out-of-plane displacements were recorded from different positions with different magnifications. Wang and Chiang [6] integrated a new interferometric arrangement with conventional moiré interferometry but their method required a light source having a relatively long temporal coherence length for the measurement of the out-of-plane component. None of these systems allowed sensitivity to be varied without replacing specimen gratings or repositioning optics.

Diffractive optic interferometry, on the other hand, has been used to measure in-plane and out-of-plane displacement components with variable sensitivity [7].

Diffractive Optic Interferometry

Figure 1 shows the experimental set-up used to illustrate three-dimensional displacement measurement using DOI. A collimated laser beam is used to illuminate a transmission grating having a structure similar to the reflective grating deposited on the specimen. As opposed to the interferometrically generated gratings applied to specimens for moiré interferometry, the gratings are binary optical elements which produce multiple diffraction orders of nearly equal intensity. The transmission grating diffracts the incoming beam to produce a number of different outgoing wavefronts. The collimated beams corresponding to the desired diffraction orders are allowed to separate until each beam can be reflected to the specimen using a different mirror. When the mirrors are properly positioned and aligned, the specimen grating recombines these beams along the normal to the surface where a digitizing camera is positioned for viewing.

Analysis

Figure 2 shows a schematic of the reflective specimen grating. For simplicity, the grating is assumed to have lines in only one direction, and the number of illuminating beams has been restricted to four. The grating is designed so that each illumination produces a diffracted wavefront normal to the surface. In the figure, unit vectors $\hat{e}_n$, $\hat{e}_m$, $\hat{e}_{-n}$, and $\hat{e}_{-m}$ represent the illumination directions while $\hat{e}_{obs}$ lies along the direction of observation. When the specimen is illuminated symmetrically with two beams, say ±n, the grating diffracts a portion of the wavefronts along the normal to the surface. Each diffracted beam acts as a reference for the other and

their superposition is equivalent to recording a hologram of the object in its undeformed state. The phase-displacement equation which governs the superposition is given by,

$$(\hat{e}_{-n} - \hat{e}_n) \cdot \underline{d} = \underline{g} \cdot \underline{d} = N\lambda \qquad (1)$$

where $\underline{d}$ is the displacement vector of a point on the object's surface, $\underline{g}$ is the sensitivity vector, N is the fringe order, and λ is the wavelength.

Equation 1 shows that displacement is measured perpendicular to the angle bisector of the illuminating beams along a direction parallel to the plane formed by them. In terms of the Cartesian coordinate system shown in Fig. 2, the unit vectors in the direction of illumination are,

$$\hat{e}_{\pm n} = \mp \sin\alpha_n \underline{i} - \cos\alpha_n \underline{k} \quad . \qquad (2)$$

Substitution of Eq. 2 into Eq. 1 gives

$$u = \frac{N\lambda}{2\sin\alpha_n} \qquad (3)$$

where u is the displacement component along the x direction and α_n is the diffraction angle corresponding to either the $\pm n$ order. The displacement is measured perpendicular to the lines in the specimen grating at a sensitivity equivalent to that which would be obtained in geometric moiré by using a grating having a pitch of $\lambda/(2\sin\alpha_n)$. The larger the angle of incidence, the greater the sensitivity.

The process of illuminating a linear diffraction grating on the surface of the specimen with two symmetrical beams is similar to the well known technique of moiré interferometry. The difference is that, since the gratings used for that technique are produced interferometrically, the value of n in Eq. (3) is restricted to 1. Hence, one advantage of using the binary optical elements is that they make it possible to vary the sensitivity after the specimen grating has been applied to the surface. More importantly, however, other combinations of orders are possible.

Consider, for example, superimposing two different pairs of symmetrical orders. Following the arguments presented for Eqs. 1 and 2, the phase differences for the pairs [n, m] and [$-n$, $-m$] are given by,

$$\begin{aligned}(\hat{e}_n - \hat{e}_m) \cdot \underline{d} &= [(-\sin\alpha_n \underline{i} - \cos\alpha_n \underline{k}) \\ &- (-\sin\alpha_m \underline{i} - \cos\alpha_m \underline{k})] \cdot \underline{d} = N_{nm}\lambda\end{aligned} \qquad (4)$$

and

$$\begin{aligned}(\hat{e}_{-n} - \hat{e}_{-m}) \cdot \underline{d} &= [(\sin\alpha_n \underline{i} - \cos\alpha_n \underline{k}) \\ &- (\sin\alpha_m \underline{i} - \cos\alpha_m \underline{k})] \cdot \underline{d} = N_{-n-m}\lambda\end{aligned} \qquad (5)$$

respectively. A moiré pattern is generated when these patterns are viewed simultaneously and the effect can be enhanced by adding a common carrier to each pattern. The governing equation is given by the difference between Eqs. 4 and 5 as,

$$u = \frac{N_D\lambda}{2(\sin\alpha_n - \sin\alpha_m)} \qquad (6)$$

where N_D is the moiré fringe order representing the difference between the fringe patterns created by the pairs. The closer the orders, the lower the sensitivity.

A second moiré pattern corresponding to the sum of Eqs. 4 and 5 can be obtained by adding an equal and opposite carrier to the two different ordered pairs. In this case, the moiré pattern is governed by,

$$w = \frac{N_S\lambda}{2(\cos\alpha_m - \cos\alpha_n)} \qquad (7)$$

where w is the out-of-plane displacement and N_S is the moiré fringe order representing the sum of the fringe patterns created by the pairs. Again, the closer the orders, the lower the sensitivity.

An alternate scenario is to use mixed pairs of similar orders. By superimposing the pairs [n, $-m$] and [$-n$, m],

$$\begin{aligned}(\hat{e}_n - \hat{e}_{-m}) \cdot \underline{d} &= [(-\sin\alpha_n \underline{i} - \cos\alpha_n \underline{k}) \\ &- (\sin\alpha_m \underline{i} - \cos\alpha_m \underline{k})] \cdot \underline{d} = N_{n-m}\lambda\end{aligned} \qquad (8)$$

and

$$\begin{aligned}(\hat{e}_{-n} - \hat{e}_m) \cdot \underline{d} &= [(\sin\alpha_n \underline{i} - \cos\alpha_n \underline{k}) \\ &- (-\sin\alpha_m \underline{i} - \cos\alpha_m \underline{k})] \cdot \underline{d} = N_{-nm}\lambda \quad .\end{aligned} \qquad (9)$$

In this case, the moiré patterns corresponding to the difference and the sum are,

$$u = \frac{N_D\lambda}{2(\sin\alpha_n + \sin\alpha_m)} \qquad (10)$$

and

$$w = \frac{N_S\lambda}{2(\cos\alpha_m - \cos\alpha_n)} \qquad (11)$$

respectively. Note that the sensitivity to in-plane displacement is enhanced by choosing a larger difference between n and m and that Eq. 11 is the same as Eq. 7. The advantage of using this approach to measure in-plane displacement, as opposed to the more conventional approach which relies on a symmetrical illumination, is that a comparable sensitivity can be achieved by illuminating the specimen at smaller angles. This enables the system to be made more compact.

Higher sensitivity to the out-of-plane displacement may be achieved by placing a partially reflecting mirror in the line of sight and then recording two symmetrical orders separately with the zero order. For the pairs [n, 0] and [$-n$, 0],

$$\begin{aligned}(\hat{e}_n - \hat{e}_0) \cdot \underline{d} &= [(-\sin\alpha_n \underline{i} - \cos\alpha_n \underline{k}) \\ &- (-\underline{k})] \cdot \underline{d} = N_{n0}\lambda\end{aligned} \qquad (12)$$

and

$$\begin{aligned}(\hat{e}_{-n} - \hat{e}_0) \cdot \underline{d} &= [(\sin\alpha_n \underline{i} - \cos\alpha_n \underline{k}) \\ &- (-\underline{k})] \cdot \underline{d} = N_{-n0}\lambda \quad .\end{aligned} \qquad (13)$$

Superimposing to obtain the sum

$$w = \frac{N_S \lambda}{2(1 - \cos\alpha_n)} \quad . \tag{14}$$

Note that Eq. 14 is also predicted by Eqs. 7 and 11 with $\alpha_m = 0$.

Still higher sensitivity can be achieved by using the beam reflected from the splitter as a reference wavefront to record a hologram with a normal illumination and observation. The governing equation for this pattern is,

$$w = \frac{N\lambda}{2} \quad . \tag{15}$$

The sensitivity can be further enhanced by applying a method introduced by Gilbert and Herrick [8]. The procedure involves recording two double exposure holograms each recorded using one of a pair of symmetrical illuminating beams. Equal and opposite phase changes are introduced into the holographic recording between exposures so that the resulting interference patterns superimpose to produce a moiré fringe pattern corresponding to their sum. For a dual beam illumination at α_n, the moiré pattern is governed by,

$$w = \frac{N_S \lambda}{2(1 + \cos\alpha_n)} \quad . \tag{16}$$

If this approach is incorporated into the DOI system, it is theoretically possible to vary the sensitivity for both in-plane and out-of-plane displacement from 0 to the point at which fringes correspond to displacements which are multiples of $\lambda/4$; twice the sensitivity that can be achieved by using the conventional methods of moiré interferometry and normal illumination/observation holographic interferometry.

Experimental Results

The system shown in Fig. 1 was constructed using a conjugate pair of diffractive optical elements designed to produce three highly efficient higher order diffraction pairs. Each of the optical elements was oriented vertically so that diffraction occurred in the horizontal direction. A study was performed on a 50.8 mm (2 inch) diameter disk placed under diametrical compression. The 3.175 mm (0.125 inch) thick disk was machined from a sheet of cast acrylic (Lucite-L). The material has an elastic modulus of 2.9 GPa (427 ksi) and a Poisson's ratio of 0.33.

The upper row of Fig. 3 shows the *u*-displacement fields obtained with the grating aligned vertically. The disk was compressed by applying a 757 N (170 lb) load in the vertical direction. The fringe patterns, presented from left to right, were obtained by isolating the [-1,+1], [-2,+2] and [-3,+3] diffraction pairs, respectively. The lower row shows the *v*-displacement fields for the disk. Since the grating was linear, the *v*-displacement patterns could only be obtained by unloading the disk and then rotating both the disk and the loading frame. Consequently, the *v*-displacement patterns were obtained by loading the disk in the horizontal direction with the grating aligned vertically. Since the load had to be reapplied, it was slightly reduced to 623 N (140 lb) so that the fringes in the more dense patterns could be counted and compared. The principal strains were largest along the horizontal center line at the center of the disk where ε_{xx} = 2051 με and ε_{yy} = -3417 με. The stresses at this location were σ_{xx} = 3020 kPa (438 psi) and σ_{yy} = -9053 kPa (-1313 psi); the ratio of σ_{yy}/σ_{xx} agrees to within 1 percent error of the theoretical value of -3.0 [9].

A second series of tests was conducted to demonstrate that out-of-plane displacement can be measured via Eqs. 7 and 11. This was accomplished by using a centrally loaded circularly clamped plate constructed by sandwiching a 127 mm (5 inch) diameter, 3.175 mm (0.125 inch) thick acrylic disk between a retaining plate and a steel frame. The material has an elastic modulus of 2.9 GPa (427 ksi) and a Poisson's ratio of 0.33. The inner lip of the retaining plate created an effective 76.2 mm (3 inch) diameter fixed-support condition. Due to grating size limitations and the symmetrical nature of the problem, the specimen grating was replicated over one quarter of the disk.

Figure 4 shows the out-of-plane displacement fields obtained when the center of the disk was displaced outward through 0.089 mm (0.0035 inches). The patterns on the left and right were obtained by superimposing mixed and symmetrical pairs, respectively. In both cases, a vertical carrier was added to the third orders by rotating the -3 and +3 mirrors, through the same amount, but in different directions around a vertical axis. A sobel filter was also applied. The fringes should be concentric but slight perturbations occur because a perfect null field could not be achieved during the initial alignment.

Figure 5, on the other hand, shows the in-plane displacement field recorded using the second order diffraction pair. The jump discontinuities in the fringe pattern are due to misalignment suffered during the step-and-repeat process used to fabricate the specimen grating. The magnitude of the maximum in-plane displacement is 0.0086 mm (0.00034 inches); approximately one-tenth that of the maximum out-of-plane displacement. It should be pointed out, however, that the displacements extracted from Figs. 4 and 5 agree to within a few percent of theory [10].

References

[1] Basehore, M.L., Post, D., "Displacement Fields (U,W) Obtained Simultaneously by Moiré Interferometry," *Applied Optics*, 21(14): 2558-2562 (1982).

[2] Basehore, M., Post, D., "Moiré Method for In-Plane and Out-of-Plane Displacement Measurements," *Experimental Mechanics*, 21(9): 321-328 (1981).

[3] Asundi, A., Cheung, M.T., "Three-Dimensional Measurement Using Moiré Interferometry," *Strain*, 24(1): 25-26 (1988).

[4] Asundi, A., Cheung, M.T., "Moiré Interferometry for out-of-Plane Displacement Measurement," *Journal of Strain Analysis*, 21(1): 51-54 (1986).

[5] Asundi, A., Cheung, M.T., Lee, C.S., "Moiré Interferometry for Simultaneous Measurement of U,V,W," *Experimental Mechanics*, 29(3): 258-260

(1989).
[6] Wang, Y., Chiang, F.P., "New Moiré Interferometry for Measuring Three-Dimensional Displacements," *Optical Engineering*, 33(8): 2654-2658 (1994).
[7] Gilbert, J.A., Shepherd, R.L., Cole, H.J., Ashley, P.R., "Three-dimensional displacement measurement using diffractive-optic interferometry," *Optical Engineering*, 36(12): 3336-3342 (1997).
[8] Gilbert, J.A., Herrick, J.W., "Dual-Beam Holographic Deflection Measurement," *Experimental Mechanics*, 21(9): 349-354 (1981).
[9] Timoshenko, S.P., Goodier, J.N., *Theory of Elasticity*, 3rd ed., McGraw-Hill, New York, 1970.
[10] Timoshenko, S.P., *Strength of Materials: Part II Advanced Theory and Problems*, 3rd ed., D. Van Nostrand Co., Inc., New Jersey, 1956.

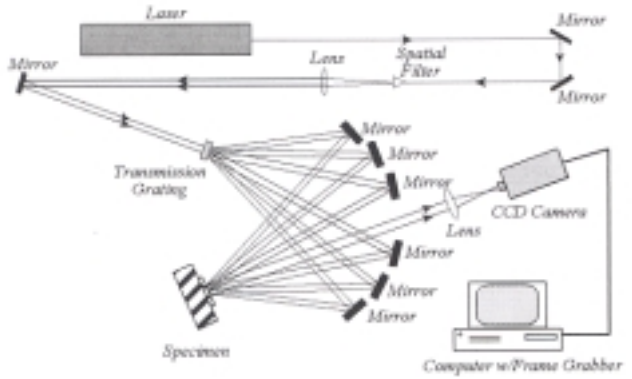

Figure 1. Experimental set-up for diffractive optic interferometry.

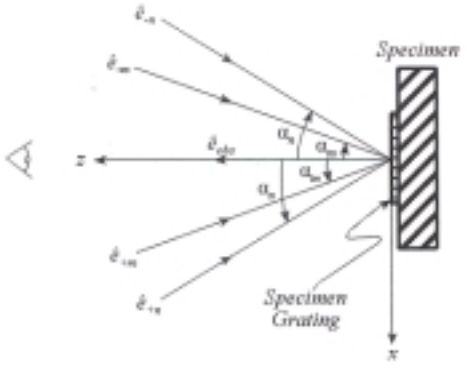

Figure 2. Multiple illumination of a diffractive optic element.

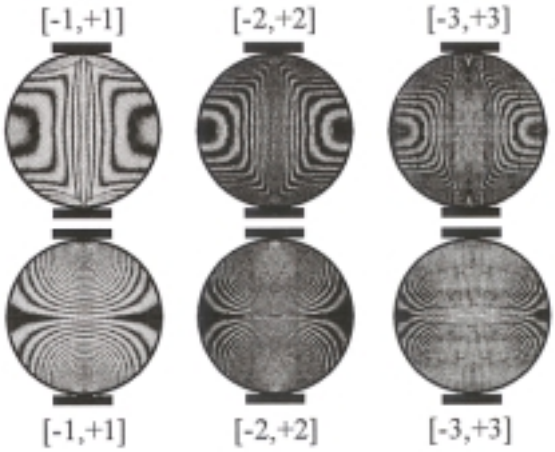

Figure 3. U (upper row) and V (lower row) displacement fields obtained from a diametrically loaded disk.

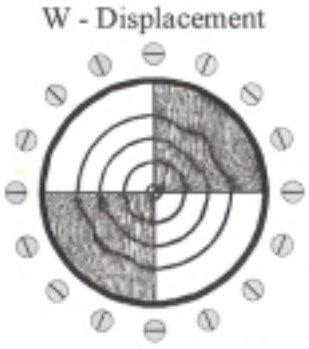

Figure 4. W-displacement fields of a centrally loaded plate.

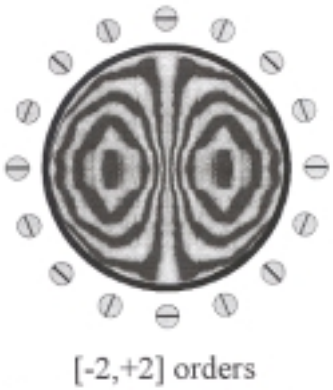

Figure 5. U-displacement field of a centrally loaded plate.